Geosmin and 2-Methylisoborneol Removal using Superfine Powdered Activated Carbon: Shell Adsorption and Branched-Pore Kinetic Model Analyse and Optimal Particle Size

Yoshihiko Matsui[1*], Soichi Nakao[2], Takuma Taniguchi[2], and Taku Matsushita[1]

Graduate School of Engineering, Hokkaido University, N13W8, Sapporo 060-8628, Japan

1 Faculty of Engineering, Hokkaido University, N13W8, Sapporo 060-8628, Japan.

2 Graduate School of Engineering, Hokkaido University, N13W8, Sapporo 060-8628, Japan.

* Corresponding Author: Phone & Fax: +81-11-706-7280, E-mail: matsui@eng.hokudai.ac.jp.

Abstract: 2-Methylisoborneol (MIB) and geosmin are naturally occurring compounds responsible for musty-earthy taste and odor in public drinking-water supplies, a severe problem faced by many utilities throughout the world. In this study, we investigated adsorptive removal of these compounds by superfine powdered activation carbon (SPAC, particle size <1 μm) produced by novel micro-grinding of powdered activated carbon; we also discuss the optimization of carbon particle size to efficiently enhance the adsorptive removal. After grinding, the absorptive capacity remained unchanged for a 2007 carbon sample and was increased for a 2010 carbon sample; the capacity increase was quantitatively described by the shell adsorption model, in which MIB and geosmin adsorbed more in the exterior of a carbon particle than in the center. The extremely high uptake rates of MIB and geosmin by SPAC were simulated well by a combination of the branched-pore kinetic model and the shell adsorption model, in which intraparticle diffusion through macropores was followed by diffusion from macropore to micropore. Simulations suggested that D_{40} was on the whole the best characteristic diameter to represent a size-disperse group of adsorbent particles; D_{40} is the diameter through which 40% of the particles by volume pass. Therefore, D_{40} can be used as an index for evaluating the improvement of adsorptive removal that resulted from pulverization. The dose required for a certain percentage removal of MIB or geosmin decreased linearly with carbon particle size (D_{40}), but the dose reduction became less effective as the activated carbon was ground down to smaller sizes around a critical value of D_{40}. For a 60-min contact time, critical D_{40} was 2–2.5 μm for MIB and 0.4–0.5 μm for geosmin. The smaller critical D_{40} was when the shorter the carbon–water contact time was or the slower the intraparticle mass transfer rate of an adsorbate was.

Keywords: Taste and odor; water treatment; PAC; SPAC; contact time

1. Introduction

For drinking water suppliers, removing any objectionable tastes and odors is key to ensuring customer satisfaction. Two important compounds, geosmin and 2-methylisoborneol (MIB), impart a strong musty-earthy taste and odor that lead to customer complaints even at concentrations as low as 10 ng/L. These compounds are the metabolites of various microorganisms, including cyanobacteria. Japan's drinking water quality standard regulates geosmin and MIB concentrations in tap water to be lower than 10 ng/L each; this is the lowest concentration level among other constituents. Effective and accepted treatment options to control taste and odor compounds include ozone oxidation and adsorption using granular or powdered activated carbon (PAC). Among these options, PAC treatment is the simplest method and perhaps the most widely applied (e.g. Srinivasan and Sorial, 2011), but is rather expensive compared to conventional treatment processes such as coagulation treatment, in particular when it is used on a continuous basis. A key difficulty with PAC is that the adsorption of MIB and geosmin is relatively slow. A very long PAC–water contact time is essential to utilize the PAC's full adsorptive capacity (Huang et al., 1996; Gillogly et al., 1998; Cook et al., 2001); alternatively, a higher dose of PAC can be used, but this increases treatment cost.

PAC's effectiveness as an adsorbent is influenced by various characteristics, including its surface chemistry, pore structure, and particle size. Micropore volume and oxygen content are key properties affecting the equilibrium adsorption capacity of activated carbon (Pendleton et al., 1997, Considine et al., 2001; Nowack et al., 2004; Yu et al., 2007; Tennant and Mazyck, 2007). Besides equilibrium capacity, adsorption kinetics is another important aspect of adsorptive removal, and smaller adsorbent particles have faster adsorption kinetics (e.g., Najm et al., 1990). Accordingly, reducing particle size to improve PAC's adsorbate uptake rate is one measure to more efficiently utilize its adsorptive capacity. Although adsorption kinetics can be enhanced by reducing the activated carbon particle

size, the overall adsorption capacity is unaffected by particle size because adsorption occurs in the internal pores of the activated carbon particles (Letterman et al., 1974; Peel and Benedek, 1980; and Leenheer, 2007). However, the recent advent of superfine powdered activated carbon (SPAC) has renewed discussions on the relationship between particle size and adsorption capacity as well as it has prompted new discussions on the relationship in the sub-micron domain (Matsui et al., 2004, 2005; Heijman et al., 2009). Smaller activated carbon particles have been reported to have greater adsorption capacity for some macromolecules, including natural organic matter (NOM); the dependency of adsorption capacity on adsorbent size is well described by the shell adsorption model (SAM; Ando et al., 2010; Matsui et al., 2011). SPAC is also superior to PAC in removing geosmin and mitigating membrane fouling when it is used in adsorption pretreatment before microfiltration (Matsui et al., 2007, 2009; Huang et al., 2009).

The homogeneous surface diffusion model (HSDM) has traditionally been used to predict the effect of adsorbent particle size on kinetics (Huang et al., 1996, Cook et al., 2001, Newcombe and Cook, 2002). However, HSDM does not accurately describe geosmin adsorption on adsorbents of different particle sizes, such as SPAC and PAC, unless the model is modified to vary surface diffusivity according to changes in carbon particle size (Matsui et al., 2009). Therefore, HSDM does not truly predict the effect of carbon particle size on adsorptive removal. The branched-pore kinetic model (BPKM), which consists of macropore diffusion followed by mass transfer from macropore to micropore, accurately describes the adsorption kinetics on SPAC and PAC with the same set of model parameter values, including surface diffusivity. In a previous study (Matsui et al., 2009), BPKM was used in conjunction with the Freundlich isotherm equation, and the adsorption isotherms of SPAC and PAC were assumed to be the same. However, the use of BPKM to model adsorption kinetics on the assumption that the adsorption capacities of SPAC and PAC are different has not been tested. Moreover, BPKM has not been applied to the removal of MIB or MIB/geosmin in natural water

systems. The relationship between MIB and geosmin removal rates and adsorbent particle size has not yet been fully analyzed, particularly in the micron and submicron range.

In the present study, we performed adsorption equilibrium and kinetics experiments to assess the capacity and the rate of MIB and geosmin uptake onto SPAC and PAC, both in the presence of NOM and in single-solute systems. To consider the effects of carbon particle size on both adsorption capacity and kinetics, we applied BPKM in conjunction with SAM. In this paper we discuss the effects of activated carbon particle size, as well as optimum particle size.

2. Materials and methods

2.1. Activated carbon

Commercially available wood-based PAC (Taikou-W, Futamura Chemical Industries Co., Gifu, Japan) was obtained in the years 2007 and 2010. SPAC was prepared by pulverizing PAC in a wet bead mill (Metawater Co., Tokyo, Japan). Both PAC and SPAC samples were slurried in ultrapure water and were stored at 4 °C. In this paper, we refer to the as-received PAC obtained in 2007 as PAC07 and that obtained in 2010 as PAC10. The pulverized carbons are referred to similarly as SPAC07 and SPAC10. We also prepared another set of pulverized carbons with median diameters between those of PAC and SPAC; these are referred to as SPACb07 and SPACb10. Particle size distributions of the activated carbon samples were determined using a laser-light scattering instrument (LA-700, Horiba, Kyoto, Japan); the samples were prepared for analysis by suspension of SPAC/PAC in water to make 200-mL samples containing 0.001 to 0.01% carbon, followed by addition of a dispersant (0.02 mL of an 18% solution of anionic surfactant) and ultrasonication for 4 min. Table 1 summarizes the properties of each activated carbon.

2.2. Water samples

Water containing NOM was collected from Lake Hakucho, Hokkaido, Japan. The sample was transported in polyethylene tanks and stored at 4 °C. The water was filtered through a 0.2-μm-pore membrane (DISMIC-25HP; Toyo Roshi Kaisha, Tokyo) and diluted to adjust the dissolved organic carbon concentration to ~1.5 mg/L; the diluent used for this purpose was prepared by amending ultrapure water (Milli-Q Advantage, Millipore Co.) with salts to obtain an ionic composition similar to that used in a previous study (Matsui et al., 2012). Stock solutions of MIB and geosmin were prepared by dissolving the pure chemicals (Wako Pure Chemical Industries, Osaka, Japan) in ultrapure water. The dissolution was confirmed by 0.2-μm membrane filtering. The NOM-containing waters (NOMWs) were spiked with the MIB or geosmin stock solutions to prepare samples with an initial MIB or geosmin concentration of ~1 μg/L. For single-solute MIB and geosmin experiments, the MIB or geosmin stock solution was added to ultrapure water amended with inorganic ions such that the ionic composition was similar to that of the NOMW; we refer to this water as organic-free water (OFW). All water samples were filtered through a 0.2-μm-pore membrane before use. MIB and geosmin concentrations were analyzed using a purge-and-trap concentrator coupled to a gas chromatograph equipped with a mass spectrometer (GCMS-QP2010 Plus; Shimadzu Corp., Kyoto, Japan; Aqua PT 5000 J, GL Sciences Inc., Tokyo, Japan). Dissolved organic carbon was quantified using a Model 810 carbon analyzer (Sievers Instruments, Inc., Boulder, CO, USA).

2.3. Batch adsorption tests

In adsorption equilibrium tests, 150-mL aliquots of OFW or NOMW spiked with MIB or geosmin (C_0 = ~1 μg/L) were transferred to 160-mL vials. A specified amount of SPAC/PAC was immediately added, the vials were manually shaken, and then the samples were agitated on a mechanical shaker for one week at a constant temperature of 20 °C. In a preliminary experiment, it was confirmed that MIB and geosmin adsorption equilibriums were reached within one week and that NOM adsorption nearly reached equilibrium. Several bottles that did not contain PAC or SPAC were used as control samples

to confirm that the concentrations of MIB, geosmin, and NOM changed negligibly during long-term agitation. After water samples were filtered through a 0.2-μm-pore membrane filter, the MIB and geosmin concentrations in the aqueous phase were measured. Solid-phase concentrations of each adsorbate were calculated from the mass that remained in the aqueous phase.

Adsorption kinetics was investigated with sample waters (3 L or 1 L) each containing MIB or geosmin (C_0 = ~1 μg/L) in a beaker with efficient mixing (200 rpm). After the addition of a specified amount of activated carbon suspension, aliquots were withdrawn at intervals and filtered immediately through a 0.2-μm-pore membrane filter for analysis of the aqueous MIB and geosmin concentrations.

3. Results and discussion

3.1. Equilibrium and kinetics of adsorption

Adsorption equilibrium tests were conducted for MIB and geosmin in the OFW system to compare SPAC with PAC. SPAC07 and SPACb07 had slightly greater MIB adsorption capacity than PAC07, but the difference (11%) was very small (Figure 1A). This result suggests that grinding did not effectively increase the MIB adsorption capacity of PAC07. SPAC10 and SPACb10 showed a somewhat greater increase in MIB adsorption capacity relative to that of PAC10; the capacity of SPAC10 was 27% greater than that of PAC10 (Figure 1B). For geosmin, the adsorption capacity difference was more pronounced, with the clear trend SPAC10 > SPACb10 > PAC10 (Figure 1C). We also conducted adsorption equilibrium tests by using natural water spiked with MIB or geosmin to elucidate the superiority of SPAC over PAC for removing MIB and geosmin under the influence of NOM. Adsorption isotherms of MIB in the presence of NOM show that SPAC10 had 23% more MIB adsorption capacity than PAC10 under this condition. The presence of NOM reduced the MIB adsorption capacity on SPAC by 85% while it reduced the capacity on PAC by 84% indicating that the adsorption capacities of SPAC and PAC were reduced to a similar extent by competitive adsorption of

NOM (Figure 1D). The same influence of NOM on the adsorption capacity between SPAC and PAC suggests the same loading of NOM that compete with MIB for adsorption sites. Details for the effect of NOM loading on SPAC and PAC adsorption are seen elsewhere (Matsui et al., 2012). The presence of NOM also reduced the geosmin adsorption capacities of SPAC and PAC to a similar extent (Figure 1E); as with MIB, the geosmin adsorption capacity of SPAC10 in the presence of NOM was also higher than that of PAC10.

The phenomenon that grinding carbon particles to reduce their size increased adsorption capacity is explained by means of a mechanism whereby molecules do not completely penetrate the adsorbent particle and instead preferentially adsorb near the outer surface of the particle (Ando et al., 2010), and the observed changes in adsorption isotherms according to carbon particle size are described well by SAM (see lines in Figure 1; see also Matsui et al., 2011), which was originally developed to describe the adsorption of NOM. In SAM, the adsorption capacity parameter, that is, the Freundlich *K* value, decreases linearly with distance from the external surface to a certain depth:

$$K_S(r,R) = K_0 \left[\max\left(\frac{r-R+\delta}{\delta}, 0\right)\right] \quad (1)$$

where r is the radial distance from the center of a adsorbent particle (cm), R is the adsorbent particle radius (cm); $K_S(r, R)$ is the Freundlich adsorption capacity parameter ((ng/mg)/(ng/L)$^{1/n}$), which varies as a function of radial distance r and adsorbent radius R; K_0 is the Freundlich parameter of adsorption at the external adsorbent particle surface ((ng/mg)/(ng/L)$^{1/n}$); δ is the penetration depth, or in other words the thickness of the penetration shell (cm); and n is the dimensionless Freundlich exponent.

In contrast to the adsorption equilibria, the adsorption kinetics of SPAC and PAC were extremely different: SPAC had a much faster uptake rate than PAC under every condition studied (Figure 2). In both OFW and NOMW systems, uptake rates of geosmin and MIB were improved greatly by using SPAC. For example, a 0.5 mg/L dose of SPAC removed geosmin at almost the same rate as 3 mg/L of PAC (Figure 2C). PAC would show little removal if the dosage was 0.5 mg/L, that was the same as that of SPAC, but this experiment was not conducted because the objective of the experiments was model parameter determination, where the data of little removal was ineffective.

These experimental data of adsorption kinetics were simulated by applying BPKM (Matsui et al., 2009), modified by incorporating SAM to describe the local adsorption equilibria in internal pores of the carbon particle. The original BPKM assumes radial intraparticle diffusion through macropores in an adsorbed state (surface diffusion). However, the surface diffusion scenario could not be applied in this study, because it assumes that the interior of the activated carbon particle is homogeneous. Such homogeneity implies that adsorbed molecules have migrated into adsorbent particles by Fick's first law of diffusion according to a local solid-phase concentration gradient, and that adsorbate molecules are ultimately distributed evenly across the inside surface of an adsorbent such that local solid-phase concentrations become equal. Such a scenario is inconsistent with SAM. Therefore, instead of modeling diffusion in an adsorbed state, we modeled diffusion of molecules in liquid-filled macropores (pore diffusion). Mass transfer resistance across the liquid film external to adsorbent particle surfaces was substantially neglected by giving a large value (10 cm/s) of liquid film mass transfer coefficient because it cannot be the rate-determining step in well mixed reactors (Sontheimer et al., 1988, Matsui et al., 2009).

Finally, the macropore mass balance equation is as follows:

$$\phi \frac{\partial q_{\mathrm{M}}(t,r,R)}{\partial t} = \frac{\emptyset D_{\mathrm{P}}}{\rho r^2} \frac{\partial}{\partial r}\left(r^2 \frac{\partial c_{\mathrm{M}}(t,r,R)}{\partial r}\right) - k_{\mathrm{B}}[q_{\mathrm{M}}(t,r,R) - q_{\mathrm{B}}(t,r,R)] \quad (2)$$

where t is adsorption time in the batch system (s); ϕ is the fraction of adsorptive capacity available in the macropore region (dimensionless); ρ is the adsorbent particle's density (g/L); D_{P} is the diffusion coefficient in the macropore (cm^2/s); c_{M} (t, r, R) is the liquid-phase concentration in a macropore of an adsorbent of radius R, at radial distance r and time t (ng/L); q_{M}(t, r, R) is the solid-phase concentration in a macropore of an adsorbent of radius R, at radial distance r and time t (ng/g); q_{B}(t, r, R) is the solid-phase concentration in a micropore of an adsorbent of radius R, at radial distance r and time t (ng/g); and k_{B} is the rate coefficient for mass transfer between macropores and micropores (s^{-1}).

The local adsorption equilibrium is expressed as follows:

$$c_{\mathrm{M}}(t,r,R) = \left(\frac{q_{\mathrm{M}}(t,r,R)}{K_{\mathrm{S}}(r,R)}\right)^n \quad (3)$$

The other BPKM equations can be seen elsewhere (Matsui et al., 2009).

Model simulations of both MIB and geosmin concentrations were overall successful in describing the curves of concentration vs. contact time in a batch adsorption system (see the lines in Figure 2). Therefore, once the adsorption equilibrium and kinetic model parameters are determined, one can predict the MIB and geosmin concentrations at a given carbon–water contact time and a given carbon particle size distribution. Using this model, one can evaluate the effect of carbon particle size on the concentrations of MIB and geosmin remaining after a given contact time.

3.2. Representative diameter for adsorption kinetics

With the successful application of BPKM-SAM to MIB and geosmin adsorption in OFW and NOMW systems, it becomes possible to quantitatively evaluate the optimum adsorbent diameters for MIB and geosmin removal. A complicating factor in studying adsorption is that activated carbon products typically consist of particles with a wide size distribution, and the dispersity of this distribution also varies considerably among different products and preparations. Therefore, we first investigated a characteristic particle size that would best represent the entire size distribution of any given carbon sample. If a suitable definition of characteristic size can be found, this greatly simplifies the problem and allows us to understand the group's adsorption kinetics using a single size value (Traegner, et al., 1996). Such a characteristic size should be a measure of central tendency, which is unaffected by the relatively few extreme values in the tails of the distribution. We tested several definitions of characteristic size: D_{20} (i.e., the diameter that 20% by volume of the all particles are finer than), D_{30}, D_{40}, D_{50}, and D_{60}. In selecting the best characteristic size, we created three fictitious particle size distributions (see Figure 3): a uniform distribution (uniformity coefficient of 1.0), a moderate distribution with a uniformity coefficient of 2.34 (the value was taken from the actual particle size distribution of SPACb07), and a wider size distribution with a uniformity coefficient of 7.59 (the value was taken from SPACb10).

Using BPKM-SAM, we simulated geosmin concentration decay for the three adsorbents each having different particle size distributions but all having the same characteristic size. In the case of D_{40}, the three curves were not so different (Figure 4), suggesting that the geosmin adsorption kinetics were almost the same among carbon samples whose D_{40} was the same, regardless of whether their particle size distribution was narrow or wide. The root mean square (RMS) of C/C_0 (remaining ratio) deviations between the moderate distribution with uniformity coefficient 2.34 and the wide distribution with 7.59 was 0.013, and the RMS value between the moderate distribution with 2.34 and

the uniform distribution with 1.0 was 0.024. We conducted this kind of BPKM simulation for D_{20}, D_{30}, D_{40}, D_{50}, and D_{60}, for both MIB and geosmin and in both OFW and NOMW; for MIB removal, RMS was minimized using D_{40}, whereas D_{30} was optimal for geosmin (Figure 5). Therefore, D_{40} was the best characteristic size to represent the kinetics of MIB removal (Figure 5A), whereas D_{30} was the best for geosmin removal (Figure 5B). We understand that for an adsorbate having a slow intraparticle mass transfer rate in a carbon particle, carbon fractions with small sizes, because they have relatively large external surface area, make a major contribution to adsorptive removal when contact times are limited. In such a case, one would expect that the most representative characteristic diameter would be less than the median diameter D_{50}. Because geosmin has a slower intraparticle mass transfer rate than MIB (as is indicated by the different curvatures of the concentration decay curves in Figure 2 and by the comparison of the D_P and k_S values between Panels B and C and between Panels D and E for the same carbons in the figure caption), it is reasonable that the most representative diameter for geosmin removal (D_{30}) was more heavily weighted to the smaller size fraction than that of MIB (D_{40}). There was no single best representative size to describe the adsorption kinetics, but the RMS values of D_{30} and D_{40} were not so different. Overall, D_{40} was the best, as it minimized the total RMS (Figure 5C). This representative diameter is expected to characterize adsorption kinetics well regardless of whether the size distribution is wide or narrow. Variations in size dispersity might result from variations in the type of grinder used, or the grinding time, but then this diameter could be used as an index to show whether the size was sufficiently small after grinding. In the present BPKM-SAM simulations, the particle size distribution of the adsorbent was taken into consideration, but most other research and practical applications of adsorption kinetics models assume uniform particle size to simplify calculations. We propose that D_{40} be used as a representative particle diameter in model simulations when a uniform particle size is assumed.

3.3. Optimum diameter for efficient absorption

The relationship between D_{40} and required dose was calculated through BPKM-SAM simulations. For a given contact time, the carbon dose required to effect a given removal percentage could be reduced by decreasing D_{40} (Figure 6). Between D_{40} values of 5 and 50 μm, the relationship was roughly linear; for example, the required dose was reduced by one fifth when D_{40} was decreased by one fifth. Matsui et al. (2007) compared the SPAC and PAC doses required for 60–98% geosmin removal in a system using flow-through PAC adsorption followed by microfiltration separation, and reported that the SPAC (D_{50} = 0.65 μm) dose required for a 4-min PAC–water contact time was 6 to 25% that of the PAC (D_{50} = 7.6 μm) dose for the same removal and contact time. In our analysis of geosmin removal, the corresponding dose ratio was 10% for a 90% removal (10% remaining ratio) over a 10-min contact time (Figure 6C and E). Although removal efficiencies may differ between flow-through and batch reactors, the results of the current study are generally consistent with the previous study.

In the scenarios modeled, the required dose initially decreased linearly with the particle size, but this trend leveled off as D_{40} reached a critical range (Figure 6). That is to say, for a given contact time and removal ratio, reducing the particle size to a certain degree effectively reduced the required carbon dose, but eventually further size reduction was not worthwhile. It is convenient to define a critical D_{40} value below which further grinding was not useful; we define critical D_{40} at the intersection between the line extrapolated from the linear dose decline and the constant line representing the lowest dose (for an example, see Figure 6A). As shown in Figure 7, critical D_{40} was larger for longer contact times, reflecting the fact that adsorption capacity becomes progressively more important than kinetics as contact time is increased. The critical D_{40} value for MIB removal was ~1 μm for a 10-min contact time, but the values were 2–2.5 and 3–4 μm for contact times of 60 and 180 min, respectively; critical D_{40} values for geosmin removal were ~0.2, 0.4–0.5, and 0.5–0.8 μm for contact times of 10, 60, and 180 min, respectively. As just mentioned, adsorption capacity becomes relatively more important

than kinetics as contact time increases. When contact times are long, only the large particles will fail to reach adsorption equilibrium, so only these large particles will have any potential for improvement of kinetics through particle size reduction. For these large particles, therefore, adsorption kinetics does still play a role even for longer contact times. Importance of adsorption kinetics only for large particles means that the critical D_{40} increases for longer contact times.

Critical D_{40} was smaller for geosmin than for MIB. As stated earlier, geosmin has slower intraparticle mass transfer within a carbon particle, meaning that adsorption kinetics plays a more important role in determining the necessary dose. Accordingly, within a size range below the critical D_{40} for MIB removal, continued reduction in size was irrelevant to MIB removal but continued to reduce the necessary dose for the equivalent geosmin removal. Using small adsorbent particles brought about fast adsorptive removal, but this effect became less important as contact time was increased. Overall, grinding activated carbon until its representative diameter D_{40} was a few microns was found to be an effective method for enhancing its adsorptivity and thereby enabling a reduction in its dose.

4. Conclusions

1. Owing to decreased carbon particle size, removal of MIB and geosmin over a given contact time was greatly enhanced. The change in adsorption isotherms with decreased particle size was explained by SAM. Irrespective of the adsorbent particle size, adsorption kinetics was well simulated by BPKM combined with SAM, using a given set of model parameter values.

2. BPKM-SAM simulations suggested that D_{40}, the diameter that 40% by volume of all the particles are finer than, was a suitable characteristic diameter that represented the adsorption kinetics of adsorbent particles well regardless of their size dispersity. Therefore, if a model simulation is

simplified by assuming uniform adsorbent particle size, we propose that D_{40} be used as the representative diameter.

3. The activated carbon dose required to effect a certain removal percentage was reduced in proportion to carbon particle size represented by D_{40}, but this effect leveled off as D_{40} fell below a certain size. This critical D_{40} value depended on the carbon–water contact time and the intraparticle mass transfer rate of adsorbate in a carbon particle; these factors determine the relative importance of adsorption capacity and kinetics on adsorptive removal.

4. Because of the kinetics enhancements that smaller particles provide, the merit of reducing particle size through grinding continued into a smaller size domain for systems that used shorter carbon–water contact times. Similarly, because geosmin was adsorbed more slowly than MIB, further reductions in particle size beyond MIB's leveling-off point continued to have greater merit for geosmin removal. The critical D_{40} values of MIB were ~1 and 3–4 μm for 10- and 180-min contact times, respectively, whereas those of geosmin were ~0.2 and 0.5–0.8 μm, respectively. Overall, grinding activated carbon until its representative diameter D_{40} was a few microns improved the speed of MIB and geosmin removal and/or reduced the needed dose over a wide range of conditions.

Acknowledgements

This study was supported by Grant-in-Aid for Scientific Research A (21246083) and S (24226012) from the Japan Society for the Promotion of Science; by Health and Labour Sciences Research Grant (Research on Health Security Control) of Japan; and by Metawater Co., Tokyo, Japan.

REFERENCES

Ando N., Matsui Y., Kurotobi R., Nakano Y., Matsushita T. and Ohno K. (2010). Comparison of natural organic matter adsorption capacities of super-powdered activated carbon and powdered activated carbon. Water Research 44 (14), 4127–4136.

Considine R., Denoyel R., Pendleton P., Schumann R. and Wong S.-H. (2001). The influence of surface chemistry on activated carbon adsorption of 2-methylisoborneol from aqueous solution. Colloids and Surfaces A: Physicochemical and Engineering Aspects 179 (2), 271–280.

Cook, D., Newcombe, G. and Sztajnbok, P. (2001) The application of powdered activated carbon for MIB and geosmin removal: Predicting PAC doses in four raw waters. Water Research 35(5), 1325-1333.

Gillogly T. E. T., Snoeyink V. L., Elarde J. R., Wilson C. M. and Royal E. P. (1998). ^{14}C-MIB adsorption on PAC in natural water. Journal of the American Water Works Association 90 (1), 98–108.

Heijman S. G. J., Hamad J. Z., Kennedy M. D., Schippers J. and Amy G. (2009). Submicron powdered activated carbon used as a pre-coat in ceramic micro-filtration. Desalination & Water Treatment 9, 86–91.

Huang C., VanBenschoten J. E. and Jensen J. N. (1996). Adsorption kinetics of MIB and geosmin. Journal of the American Water Works Association 88 (4), 116–128.

Huang, H., Schwab, K. and Jacangelo, J.G. (2009) Pretreatment for low pressure membranes in water treatment: a review. Environmental Science & Technology 43(9), 3011-3019.

Leenheer J.A. (2007). Progression from model structures to molecular structures of natural organic matter components. Annals of Environmental Science 1, 57–68.

Letterman R.D., Quon J.E. and Gemmell R.S. (1974). Film transport coefficient in agitated suspensions of activated carbon. Journal of the Water Pollution Control Federation 46 (11), 2536–2547.

Matsui Y., Fukuda Y., Murase R., Aoki N., Mima S., Inoue T. and Matsushita T. (2004). Micro-ground powdered activated carbon for effective removal of natural organic matter during water treatment. Water Science and Technology: Water Supply 4 (4), 155–163.

Matsui Y., Murase R., Sanogawa T., Aoki N., Mima S., Inoue T. and Matsushita T. (2005). Rapid adsorption pretreatment with submicrometre powdered activated carbon particles before microfiltration. Water Science and Technology 51 (6–7), 249–256.

Matsui Y., Aizawa T., Kanda F., Nigorikawa N., Mima S. and Kawase Y. (2007). Adsorptive removal of geosmin by ceramic membrane filtration with super-powdered activated carbon. Journal of Water Supply: Research and Technology-AQUA 56 (6–7), 411–418.

Matsui Y., Ando N., Sasaki H., Matsushita T. and Ohno K. (2009). Branched pore kinetic model analysis of geosmin adsorption on super-powdered activated carbon. Water Research 43 (12), 3095–3103.

Matsui, Y., Hasegawa, H., Ohno, K., Matsushita, T., Mima, S., Kawase, Y. and Aizawa, T. (2009) Effects of super-powdered activated carbon pretreatment on coagulation and trans-membrane pressure buildup during microfiltration. Water Research 43(20), 5160 –5170.

Matsui Y., Ando N., Yoshida T., Kurotobi R., Matsushita T. and Ohno K. (2011). Modeling high adsorption capacity and kinetics of organic macromolecules on super-powdered activated carbon. Water Research 45 (4), 1720–1728.

Matsui Y., Yoshida T., Nakao S., Knappe D. R. U. and Matsushita T. (2012). Characteristics of competitive adsorption between 2-methylisoborneol and natural organic matter on superfine and conventionally sized powdered activated carbons. Water Research 46(15), 4741-4749. .

Najm I., Snoeyink V. L., Suidan M. T., Lee C. H. and Richard Y. (1990). Effect of particle size and background natural organics on the adsorption efficiency of PAC. Journal of the American Water Works Association. 82 (1), 65–72.

Newcombe, G. and Cook, D. (2002) Influences on the removal of tastes and odours by PAC. Journal of Water Supply Research and Technology-AQUA 51(8), 463-474.

Nowack, K. O., Cannon, F. S. and Mazyck, D. W. (2004) Enhancing Activated Carbon Adsorption of 2-Methylisoborneol: Methane and Steam Treatments. Environmental Science & Technology 38(1), 276-284.

Peel R.G. and Benedek A. (1980). Attainment of equilibrium in activated carbon isotherm studies. Environmental Science and Technology 14 (1), 66–71.

Pendleton, P. , Wong, S. H., Schumann, R., Levay, G., Denoyel, R. and Rouquero, J. (1997) Properties of activated carbon controlling 2-Methylisoborneol adsorption. Carbon 35(8), 1141-1149.

Tennant, M. F. and Mazyck, D. W. (2007) The role of surface acidity and pore size distribution in the adsorption of 2-methylisoborneol via powdered activated carbon. Carbon 45(4), 858-864.

Traegner, U. K., Suidan, M. K. and Kim, B. R. (1996) Considering age and size distributions of activated-carbon particles in a completely-mixed adsorber at steady state. Water Research 30(6), 1495-1501.

Srinivasan R. and Sorial G. A. (2011). Treatment of taste and odor causing compounds 2-methyl isoborneol and geosmin in drinking water: A critical review. Journal of Environmental Sciences 23 (1), 1–13.

Yu, J., Yang M., Lin T.-F., Guo Z., Zhang Y., Gu J. and Zhang S. (2007). Effects of surface

characteristics of activated carbon on the adsorption of 2-methylisobornel (MIB) and geosmin from natural water. Separation and Purification Technology 56 (3), 363–370.

Table 1. Size and surface area characteristics of the activated carbon particles studied.

Sample name	Median diameter (D_{50}, μm)	Effective diameter (D_{10}, μm)	Uniformity coefficient	Geometric standard deviation	BET surface area (m^2/g)
PAC07	11.8	3.89	3.27	2.27	1170
SPACb07	1.91	0.904	2.34	1.85	n/a
SPAC07	0.725	0.271	3.15	1.93	1110
PAC10	13.5	3.35	5.19	2.80	1070
SPACb10	4.87	0.853	7.59	3.29	n/a
SPAC10	0.857	0.396	2.70	3.00	1130

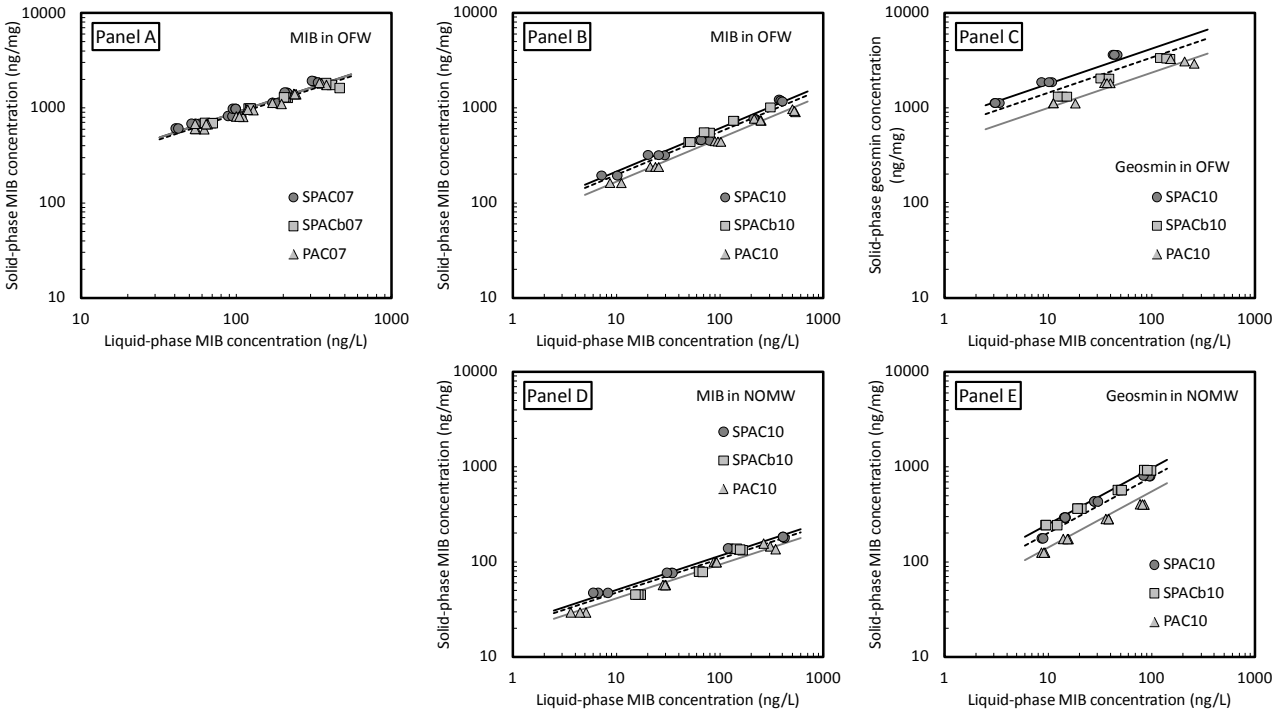

Fig. 1. Adsorption isotherms for MIB (Panels A, B, and D) and geosmin (Panels C and E). Experimental data are shown as points, and SAM fits to the data are shown as lines. The SAM fit parameters are as follows:
Panel A — K_0: 3.1 (mg/g)/(ng/L)$^{1/n}$, δ: 38.6, 1/n: 0.54
Panel B — K_0: 1.8 (mg/g)/(ng/L)$^{1/n}$, δ: 9.1, 1/n: 0.46
Panel C — K_0: 10.7 (mg/g)/(ng/L)$^{1/n}$, δ: 3.0, 1/n: 0.37
Panel D — K_0: 0.3 (mg/g)/(ng/L)$^{1/n}$, δ: 11.0, 1/n: 0.36
Panel E — K_0: 4.1 (mg/g)/(ng/L)$^{1/n}$, δ: 3.2, 1/n: 0.59.

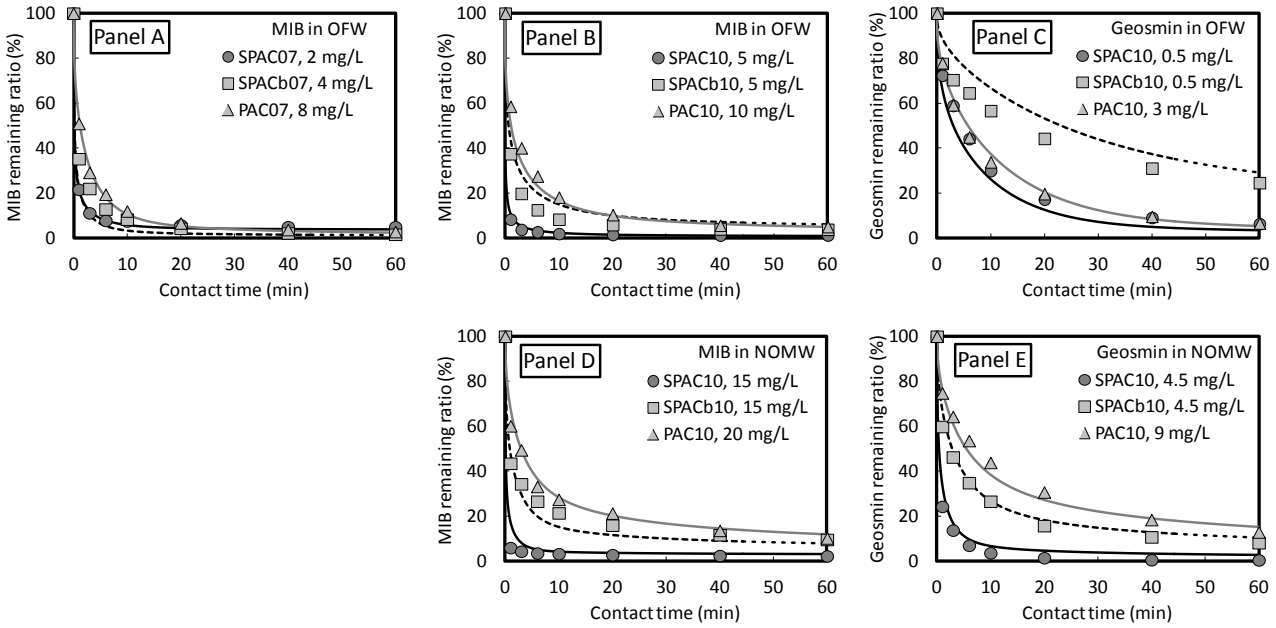

Fig. 2. Adsorption kinetics for MIB (Panels A, B, and D) and geosmin (Panels C and E). Experimental data are shown as points, and BPKM-SAM simulations are shown as lines. Initial MIB and geosmin concentrations are ~1 μg/L. The BPKM-SAM parameters are as follows:
Panel A — D_P: 1.7×10^{-7} cm^2/s, k_S: 8.7×10^{-4} s^{-1}, ϕ: 0.57
Panel B — D_P: 3.1×10^{-7} cm^2/s, k_S: 3.9×10^{-4} s^{-1}, ϕ: 0.73
Panel C — D_P: 2.1×10^{-7} cm^2/s, k_S: 3.8×10^{-4} s^{-1}, ϕ: 0.29
Panel D — D_P: 3.0×10^{-7} cm^2/s, k_S: 2.1×10^{-3} s^{-1}, ϕ: 0.55
Panel E — D_P: 0.44×10^{-7} cm^2/s, k_S: 1.5×10^{-3} s^{-1}, ϕ: 0.53.

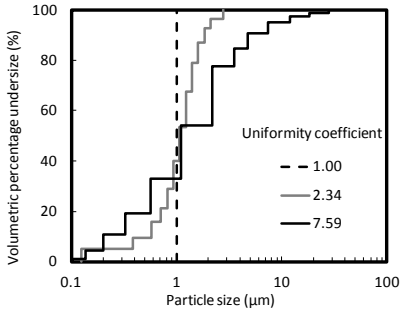

Fig.3. Fictitious adsorbent particle size distributions with the same D_{40} (1.0 μm) for BPKM-SAM simulations.

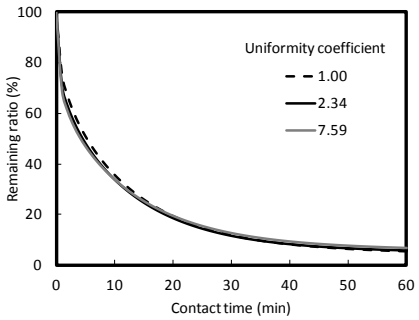

Fig. 4. Effect of particle size distribution on adsorption kinetics of geosmin: BKAM-SAM simulations (D_{40} = 1.0 μm, activated carbon dose = 0.5 mg/L, initial geosmin concentration: 1000 ng/L, NOM water, D_S: 2.1×10^{-7} cm^2/s, k_S: 3.8×10^{-4} s^{-1}, ϕ: 0.29).

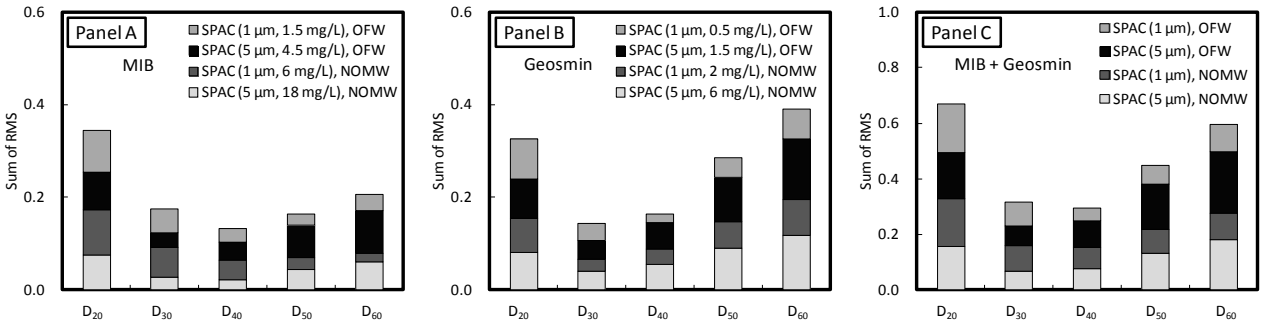

Fig. 5. Sums of root mean square (RMS) values to select the best characteristic size that represents a group of adsorbent particles with the same size distribution (Initial MIB or geosmin concentration is 1000 ng/L).

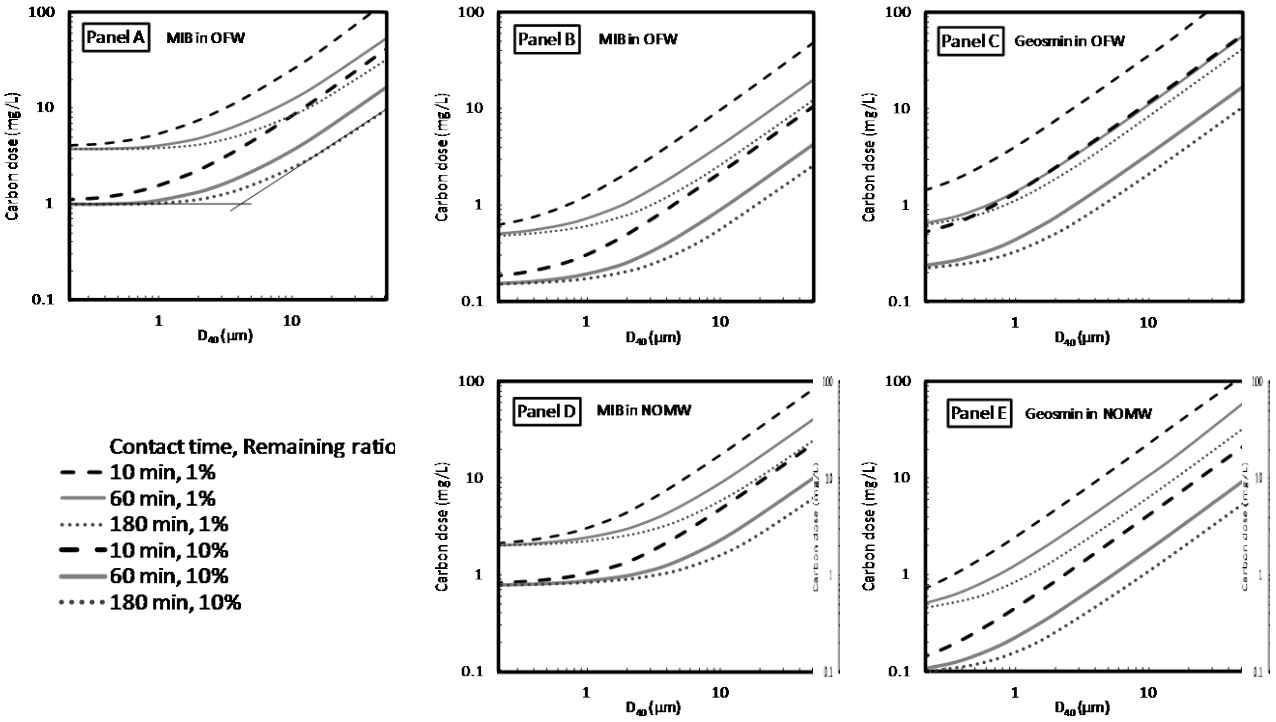

Fig. 6. Dose required for various removal percentages and contact times vs. particle size of activated carbon for MIB (Panels A, B, and D) and geosmin (Panels D and E) removal: PBKM-SAM simulations. Initial concentration is 1000 ng/L. PBKM-SAM parameter values are the same as those of Figures 1 and 2. Panel A: Carbon sample from the year 2007. Panels B−E: Carbon sample from the year 2010.

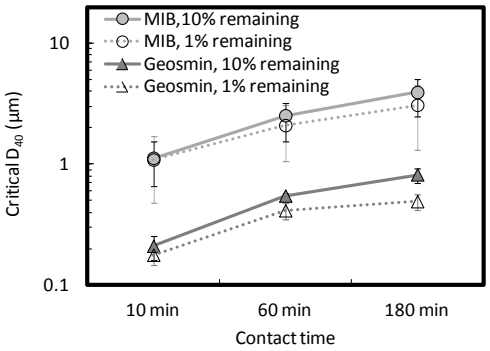

Fig. 7. Effect of carbon−water contact time on the critical D_{40} value.